Observation of magnonic band gaps in magnonic crystals with nonreciprocal dispersion relation

M. Mruczkiewicz,[1,*] E. S. Pavlov,[2] S. L. Vysotsky,[2] M. Krawczyk,[1,*] Yu. A. Filimonov,[2,3] and S. A. Nikitov[3,4,5]

[1]*Faculty of Physics, Adam Mickiewicz University in Poznan, Umultowska 85, Poznań 61-614, Poland*

[2]*Kotel'nikov Institute of Radio-Engineering and Electronics of RAS, Saratov Branch, Zelenaya Street 38, Saratov 410019, Russia*

[3]*Saratov State University, Astrakhanskaya Street 83, Saratov 410012, Russia*

[4]*Kotel'nikov Institute of Radio-Engineering and Electronics of RAS, Mokhovaya Street 11, Building 7, Moscow 125009, Russia*

[5]*Moscow Institute of Physics and Technology, Dolgoprudny 141700, Moscow Region, Russia*

(Received 14 August 2014; revised manuscript received 29 October 2014; published 14 November 2014)

An effect of metallization of a magnonic crystal surface on band-gap formation in the spectra of a surface spin wave (SSW) is studied both theoretically and experimentally. The structures under consideration are one-dimensional magnonic crystals based on yttrium iron garnet with an array of etched grooves, with and without a metal screen on the top of the corrugated surface. Due to nonreciprocity of propagation of the SSW, the shift of the band gap to higher frequency and from the border of the Brillouin zone in the presence of a conducting overlayer was measured in a transmission line experiment. Results of numerical calculations and model analysis are in agreement with experimental data and give further insight into the origin of the band gap and properties of the nonreciprocal SSW in metalized magnonic crystals. This gives a positive answer to the outstanding question about the possibility of detection of magnonic band gaps in the spectra of spin waves with nonreciprocal dispersion in magnonic crystals, and creates the potential for new applications and improvements of already existing prototype magnonic devices.

DOI: 10.1103/PhysRevB.90.174416 PACS number(s): 75.40.Gb, 75.25.−j, 75.30.Ds, 75.40.Mg

The surface spin waves (SSWs) propagating in a ferromagnetic film along the direction perpendicular to a tangentially applied magnetic field $\boldsymbol{H_0}$ (Damon-Eshbach geometry) [1] posses nonreciprocal properties. More specifically, SSW amplitude distribution through the film thickness d has a maximum near opposite surfaces for waves with converse direction of the wave vector $\boldsymbol{k}$ or bias magnetic field $\boldsymbol{H_0}$, while the frequencies f of the oppositely directed waves are the same $f(k) = f(-k)$. Since for the Damon-Eshbach mode the distribution of amplitude across the thickness is nonsymmetrical with respect to the middle plane of the film, and also the distribution of the electric field is nonsymmetrical [2], nonreciprocity in dispersion [3] $f(k) \neq f(-k)$ and attenuation $\mathrm{Im}\, f(k) \neq \mathrm{Im}\, f(-k)$ [4] of the oppositely directed SSWs can appear if a metallic layer is placed near one of the ferromagnetic film surfaces. The changes in dispersion of the SSW propagating along the metalized surface can be treated in approximation as influence of an ideal metal if the thickness D of the metallic layer satisfies the condition $D > 3k\rho$ [5], where ρ is the skin depth of the metal at the SSW frequencies. In this case nonreciprocity in dispersion $f(k) \neq f(-k)$ manifests itself not only in changes of the dispersion slope of SSWs propagating along the metalized surface, but for sufficiently small thickness t of the dielectric spacer between metallic and magnetic layers ($t < 2d$) it leads to expanding of the SSW bandwidth on some value $\Delta\Omega$ above the frequency range of SSWs traveling along the free surface [6]. At frequencies $\Delta\Omega$ propagation of SSWs is unidirectional (possible only along metalized surface), which can be used for wave steering and channeling control [7] and suppression of the spatial resonances [8]. The SSW propagation in metalized magnetic films was also studied from the point of view of the signal delay line design [9] and soliton formation [10].

*Corresponding authors: m.mru@amu.edu.pl, krawczyk@amu.edu.pl

Since magnonic crystals (MCs) attract wide attention of researchers due to their usefulness for manipulation of spin wave band structures [11–17], it is natural that the influence of metallization on MCs was also recently investigated. In the previous studies it was shown experimentally that the band gap at the frequency of an unmetalized structure disappears when the metallic plate is attached [18]. However, at that time theoretical predictions that the gaps appear at a higher frequency range were not available yet [19,20]. Here we present an experimental demonstration of the nonreciprocal dispersion relation of spin waves and the existence of an indirect magnonic band gap in one-dimensional magnonic crystals in contact with a metallic film.

The nonreciprocal properties of magnonic band structure are potentially useful for designing miniaturized microwave isolators and circulators, essential elements in microwave technology. The structure based on a uniform yttrium iron garnet (YIG) film with metallic stripes was proposed as an ultrasensitive magnetic field sensor [21]. Although not considered in that study, the nonreciprocal properties of SSWs can influence positively their sensitivity. The nonreciprocity can be also of big importance for magnonics, where spin waves are used to process information [22,23]. The dispersion of metal-YIG structures is also an important factor for electrically tunable magnonic devices [24]. The technologically simple design proposed here can be of advantage over other complicated magnonic crystal based nonreciprocal structures [25]. Moreover, the influence of metal in the surrounding space of a magnonic device, especially when integrated, can additionally result in changes of its functionality [26,27].

Here, we investigate the influence of a metal on the magnonic band structure in two microscale MCs made of YIG films with etched grooves. The structure under consideration is depicted in Fig. 1. The YIG films were grown on a ⟨111⟩-oriented gadolinium gallium garnet (GGG) substrate. The grooves were introduced by chemical etching on the YIG surface, which formed a periodic structurization. The first MC

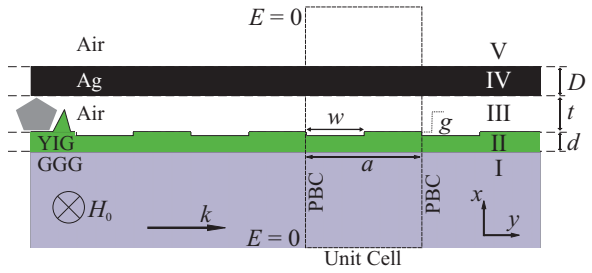

FIG. 1. (Color online) A schema of the structure under consideration. The materials are indicated as follows: (I) dielectric substrate (GGG), (II) magnonic crystal (YIG), (III) air gap, (IV) metallic overlayer (Cu), and (V) air surrounding. The bias magnetic field H_0 is in the film plane and directed along the z axis. The SSWs propagate along the y axis. The rectangular unit cell used in numerical calculations is marked by the dashed line. The periodic boundary conditions (PBCs) were used along the y axis. The bottom and top borders of the unit cell are far from the structure; at these borders we assume fields equal 0. The irregularities of the YIG film and dust particles are indicated schematically as the green triangle and gray pentagon, respectively.

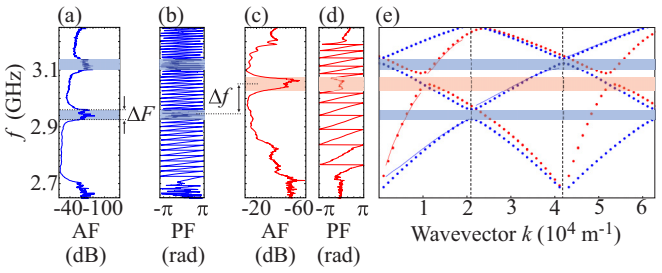

FIG. 3. (Color online) Result of the measurements for sample I ($a = 150$ μm). (a) Amplitude-frequency (AF) and (b) phase-frequency (PF) characteristics of YIG MC without metal overlayer; (c) AF and (d) PF characteristics of YIG MC with metal overlayer. (e) The comparison of dispersion relations obtained from numerical calculations (blue dots for unmetalized sample, red dots for metalized) and from measured PF signal (blue lines for unmetalized sample and red lines for metalized). The transparent blue and red bars indicate experimentally measured positions of magnonic band gaps in unmetalized and metalized samples, respectively. The vertical dashed lines in (e) indicate the edges of Brillouin zones, Δf is the frequncy shift of the magnonic gap induced by metallization, and ΔF is the magnonic bad gap width.

(sample I) consists of the $d \approx 7.7$ μm thick YIG film with an array of etched grooves of depth $g \approx 1.5$ μm and width $w \approx 80$ μm. The separation between grooves is approximately 70 μm and the lattice constant is $a \approx 150$ μm. The second MC (sample II) is a $d \approx 3.8$ μm thick YIG film with an array of grooves with depth $g \approx 2$ μm and width $w \approx 50$ μm. The separation between grooves is approximately 150 μm and the lattice constant is $a \approx 200$ μm. The wave vectors at the edge of the first Brillouin zone (BZ) for the investigated structures are 2×10^4 and 1.5×10^4 m^{-1}, for samples I and II, respectively. On the basis of analysis conducted in Refs. [6,20] we can expect that the effect of metallization on the magnonic gap formation ought to be observable if the thickness of the dielectric spacer t is smaller than lattice constant a ($t < a$). For the chosen structures this requirement will be fulfilled if $t \approx 100$ μm. On the other hand the air gap of such values can be easily realized experimentally [28,29].

To investigate features of magnonic band formation in spectra of nonreciprocal waves, the measurements of transmission and phase characteristics in two types of SSW delay lines based on MCs were performed. The first type was made by putting the MCs on the microstripe transducers, while in the second type coplanar transducers were used; see Fig. 2. Both types of transducers were prepared by using

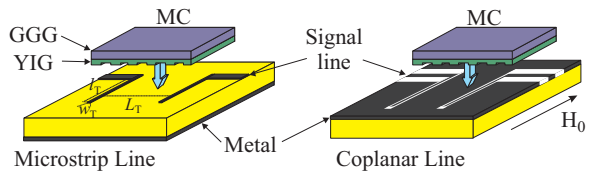

FIG. 2. (Color online) A microstrip (left) and coplanar (right) line used in the SSW transmission measurements through MCs without and with a metallic overlayer. In the experimental setup the MC sample is placed on top with the grooved side close to the transducers.

photolithography on alumina substrates covered by Cu layers with thickness $D \approx 5$ μm. Input and output transducers have width $w_T \approx 30$ μm, length $l_T \approx 4$ mm and were separated by distance $L_T \approx 4$ mm. The YIG films under investigations had planar dimensions 15 mm×5 mm. The whole structure was placed in the gap of an electromagnet so that the external magnetic field was oriented along the grooves and parallel to the transducers. The field was strong enough to saturate the sample ($\mu_0 H_0 \approx 41.6$ mT). The amplitude-frequency (AF) and phase-frequency (PF) characteristics of the delay line prototype models were measured by an Agilent E5071C-480 network analyzer. The ground layer of metal of the coplanar line serves also as a metal overlayer, depicted in Fig. 1.

Using those two different types of delay lines (microstripe and coplanar) the transmission of SSWs in MC without and with a metallic overlayer was measured for samples I and II. The measured transmission spectra (AF characteristic) are shown in Figs. 3(a) and 3(c) and in Figs. 5(a) and 5(c) for samples I and II, respectively. Magnonic band gaps ΔF indicated by low AF signal are found in both transmission spectra and are marked by shadowed rectangles. However, in the case of MCs with metallic overlayer [Figs. 3(c) and 5(c)] the first magnonic gap is shifted to the higher frequencies by some value Δf; see Figs. 3(e) and 5(e). The frequency shift was $\Delta f \approx 120$ MHz and $\Delta f \approx 140$ MHz for samples I and II, respectively. The existence of these gaps is confirmed also in the respective PF characteristics which are presented in Figs. 3(b) and 3(d) and Figs. 5(b) and 5(d) for samples I and II, respectively.

In order to obtain more insight into the formation of the magnonic band gaps in the nonreciprocal structure, the numerical calculations of the dispersion relation were performed. For SSWs from the GHz frequency range, a large value of the thickness of MCs considered in the paper, and a small value of the exchange constant of YIG, the magnetostatic approximation is well justified. Therefore, the

exchange coefficient in YIG is neglected in our theoretical investigation. In order to calculate the SSW dispersion relation we solved the wave equation for an electric field vector **E** [30]:

$$\nabla \times \left(\frac{1}{\hat{\mu}(\mathbf{r})} \nabla \times \mathbf{E} \right) - \omega^2 \sqrt{\epsilon_0 \mu_0} \left(\epsilon_0 - \frac{i\sigma}{\omega \epsilon_0} \right) \mathbf{E} = 0, \quad (1)$$

where $\omega = 2\pi f$, μ_0 and ϵ_0 denote the vacuum permeability and permittivity, respectively, and σ is the conductivity, different from zero only in the metallic overlayer. To describe the dynamics of the microwave magnetization components perpendicular to the external magnetic field, it is sufficient to solve Eq. (1) for the z component of the electric field vector **E** which depends solely on x and y coordinates [2]: $E_z(x,y)$. The MCs under consideration are assumed infinite along the z direction. The permeability tensor $\hat{\mu}(\mathbf{r})$ is obtained from the linearized damping-free Landau-Lifshitz equation [31]:

$$\hat{\mu}(\mathbf{r}) = \begin{pmatrix} \mu^{xx}(\mathbf{r}) & i\mu^{xy}(\mathbf{r}) & 0 \\ -i\mu^{yx}(\mathbf{r}) & \mu^{yy}(\mathbf{r}) & 0 \\ 0 & 0 & 1 \end{pmatrix}, \quad (2)$$

where

$$\mu^{xx}(\mathbf{r}) = \frac{\gamma\mu_0 H_0(\gamma\mu_0 H_0 + \gamma\mu_0 M_S(\mathbf{r})) - (2\pi f)^2}{(\gamma\mu_0 H_0)^2 - (2\pi f)^2}, \quad (3)$$

$$\mu^{xy}(\mathbf{r}) = \frac{\gamma\mu_0 M_S(\mathbf{r}) 2\pi f}{(\gamma\mu_0 H_0)^2 - (2\pi f)^2}, \quad (4)$$

$$\mu^{yx}(\mathbf{r}) = \mu^{xy}(\mathbf{r}), \quad \mu^{yy}(\mathbf{r}) = \mu^{xx}(\mathbf{r}); \quad (5)$$

M_S is the saturation magnetization of YIG and γ is the gyromagnetic ratio. Equation (1) has coefficients that are constants or periodic functions of y (with a period a), thus the Bloch theorem can be used:

$$E_z(x,y) = E'_z(x,y)e^{ik_y \cdot y}, \quad (6)$$

where $E'_z(x,y)$ is a periodic function of y: $E'_z(x,y) = E'_z(x,y+a)$. k_y is a wave vector component along y, and, due to considering SSW propagation along this direction only, we assume $k_y \equiv k$. Equation (1) together with Eq. (6) can be written in the weak form [32] and the eigenvalue problem can be generated. This eigenequation is supplemented with the Dirichlet boundary conditions at the borders of the computational area placed far from the ferromagnetic film along the x axis (dashed lines in Fig. 1). This eigenequation is solved by the finite element method with the use of the commercial software COMSOL software.

In calculations we take nominal values of the MC dimensions (for samples I and II) and the saturation magnetization of YIG as $M_S = 0.143\times10^6$ A/m and $M_S = 0.142\times10^6$ A/m for samples I and II, respectively. Note the difference in M_S can be attributed to growth of anisotropy fields which results from YIG and GGG lattice mismatch during epitaxy. The conductivity of the metal is assumed as $\sigma = 5.8\times10^7$ S/m, which is a tabular value for Cu [33].

Because the MC was put just on the top of the transducers without any polishing of the MC surface, the real separation can be in the range of a few to a dozen μm due to some irregularities or dust grains (schematically shown in Fig. 1). In addition, any irregularity of the YIG film or the metal layer will also result in an increase of this separation. It is also possible that conductivity of the metal σ or its thickness D are different than assumed in the calculations. However, the dispersion relation is not sensitive to variation of the product of conductivity and thickness of the metal, σD, at the range of SSW wave vectors of interest [34]. Thus only t was used as a free parameter in calculations. In Fig. 4 the frequency shift (Δf) of the first magnonic band gap in sample I with the metallic overlayer with respect to the MC without the metal is shown in dependence on t. For $t = 0$ the effect of metal overlayer is the largest, the group velocity of spin waves propagating along the direction of metalized surface is highest, and the largest shift of band gap is observed. Introducing separation between sample and metal results in monotonic decrease of group velocity. Therefore, there is a monotonic decrease of Δf with increasing t, because the influence of the metal decreases. The agreement with the experimental data for sample I with the metallic overlayer is achieved for $t = 18$ μm, and this value is used in the following calculations.

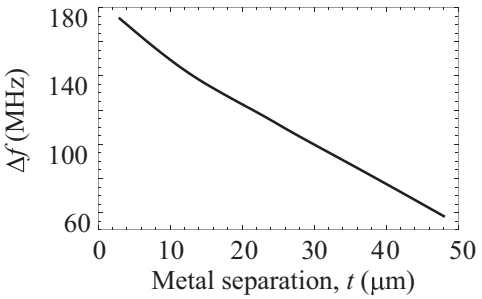

FIG. 4. The metallization induced frequency shift (Δf) of the magnonic band gap in sample I in dependence on the separation distance of the metal from the magnonic crystal surface.

In Fig. 3(e) the results of calculated dispersion relations are presented by blue and red dots for sample I without and with metallic overlayer, respectively. In this figure we can see that the edge of the magnonic band gap in the metalized structure is shifted from the border of the Brillouin zone, and this effect is due to nonreciprocity of the SSW dispersion relation. The gap opens when the interacting SSWs with equal frequencies fulfill the general Bragg condition [20]. Magnonic band gaps are marked by transparent blue and red horizontal bars for measurements with and without metallic overlayer, respectively. The size of the first magnonic gap is $\Delta F \approx 39$ MHz for the sample with metal overlayer and $\Delta F \approx 35$ MHz for the sample without metal overlayer. The position and the width of the band gaps from calculations agree very well with the gaps found in the transmission experiment. Thus, we have shown experimentally that magnonic band gaps can exist in MCs covered by a metallic overlayer in the frequency and wave vector part of the SSW spectra where nonreciprocal properties are significant.

From the measured PF characteristic we can obtain even more information about the SSW dispersion in MCs than from the AF characteristic. The PF graphs are reduced to the $-\pi$ and π values and of course the waves with phase difference 2π are not differentiable. But the phase jump over 2π phase difference visible in the PF characteristic at frequencies from a transmission band is determined by the separation distance

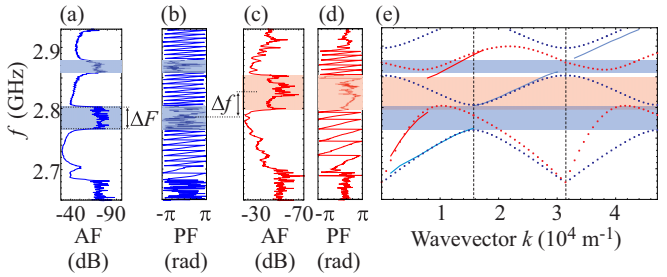

FIG. 5. (Color online) The result of measurements and calculations for sample II ($a = 200\ \mu$m). (a) AF and (b) PF characteristics of YIG MC without metal overlayer; (c) AF and (d) PF characteristics of YIG MC with metal overlayer. (e) The comparison of dispersion relations obtained from numerical calculations (blue dots for unmetalized sample, red dots for metalized) and from PF signal (blue line for unmetalized sample, red line for metalized). The transparent blue and red bars indicate experimental positions of the magnonic band gaps in unmetalized and metalized samples, respectively.

between the transducers and is related to the change of the SSW wave vector $\Delta k = 2\pi/L_T = 0.157\times10^4$ m^{-1}. This way the dispersion relation can be estimated, although ambiguously it gives clear information about the slope of the dispersion curve (i.e., its group velocity) at different parts of the magnonic spectra. Comparing Figs. 3(b) and 5(d) we can see that the group velocity of SSWs from the first and second bands in the MC with metal are much higher than respective velocities in the MC without metal. By assigning a wave number $k = n\pi/a$ for the frequency corresponding to the value of phase equal to $-\pi$ at the edge of the nth magnonic gap, we can superimpose the function $f(k)$ extracted from the PF characteristic on the calculated dispersion relation. These dispersions are presented with red and blue continuous lines in Fig. 3(e) for sample I. The agreement between measured and calculated dispersion curves is very good and proves that the metallic overlayer can be used not only to tune position of the magnonic band gap but also to mold the velocity of the transmitted signal. Moreover, the shape of the dispersion curve at the magnonic band gap edge can be an important factor for possible applications of MCs, e.g., as ultrasensitive sensors of a magnetic field [21].

Figures 5(a)–5(d) show results of measured AF and PF characteristics of unmetalized and metalized sample II. The comparison of dispersion relations extracted from the PF characteristics with the results of calculations is shown in Fig. 5(e). In this case the separation between YIG and metal was taken as $t = 28\ \mu$m. The AF and PF characteristics show wide band gaps (wider than for sample I) at different frequency ranges. The size of the first magnonic gap is $\Delta F \approx 61$ MHz for the sample with metal overlayer and $\Delta F \approx 44$ MHz for the sample without metal overlayer. It is due to the larger ratio of groove depth to YIG thickness in sample II than in sample I. Again, band gap at elevated frequencies is measured with the use of coplanar lines. The numerical dispersion relation confirms existence of a large indirect magnonic band gap and a larger group velocity of SSWs in sample II, in agreement with the dispersion extracted from the PF characteristic.

Additional calculations were performed to find influence of the lattice constant on the shift of the frequency of the magnonic band gap due to metallization. The frequency of the

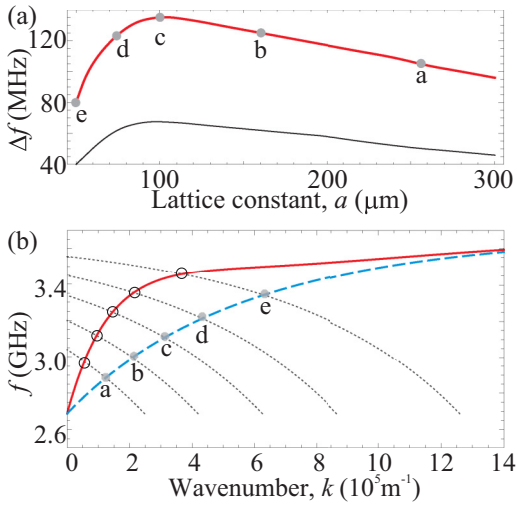

FIG. 6. (Color online) (a) Shift of the magnonic band gap frequency due to metallization as a function of the lattice constant. The thick red solid line is for YIG MC of 7.7 μm thickness and 1.5 μm deep grooves with width $w = 0.5a$. The black thin line is for YIG MC of thickness 3.8 μm and 2 μm deep grooves with width $w = 0.25a$. The separation of tmetal layer from MC was fixed to 18 μm in both cases. (b) The SSW dispersion relation of a homogeneous YIG film of 7.7 μm thickness with a metal overlayer (red solid line) and without metal (blue dashed line). The gray dotted lines are artificially introduced back-folded branches due to selected periodicities marked in (a) by letters from a to e. The small full-gray and big empty dots indicate the expected positions of the magnonic band gap in MC without (which opens at the border of the first BZ, π/a) and with metallic overlayer (inside the BZ), respectively, for selected lattice constant in (a).

band gap shift in dependence on the lattice constant for a YIG MC of 7.7 μm thickness and 1.5 μm deep grooves with width $w = 0.5a$ is shown with a bold solid red line in Fig. 6(a). The same function is also plotted for a MC of thickness 3.8 μm with 2 μm deep grooves and width $w = 0.25a$ with a thin gray line. In both cases the separation of metal from the MC surface was fixed to 18 μm. It can be seen that for MCs characterized by different thicknesses it is possible to define an optimal value of the lattice constant for which the shift of the band gap is largest.

The dependence in Fig. 6(a) can be understood by analysis of the dispersion relation of SSWs in a homogeneous YIG film shown in Fig. 6(b), where the solid red and blue dashed lines indicate the films with and without metallic overlayer, respectively. The position of the band gap in the MC can be estimated by introducing artificial periodicity into a homogeneous film and by the exploitation of the band periodicity in the wave vector space according with the Bloch theorem. Therefore, the thin dotted lines in Fig. 6(b) show dispersion relations of SSWs propagating in the $-k$ direction (i.e., unaffected by the metal film) shifted by the reciprocal lattice vector $2\pi/a$ for five selected lattice constants marked by letters a to e in Fig. 6(a). The small full dots indicate the first BZ boundary (and the location of magnonic band gap in the MC without metal) for chosen lattice constants; the big empty dots indicate the intersections of dispersion for $+k$ (solid red) with

$-k + 2\pi/a$ (i.e., the expected location of the magnonic band gaps) for the metalized MC. The observed increase of the band gap shift with decreasing lattice constant from $a = 300$ μm to 100 μm [points a, b, c in Fig. 6(a)] is because of increasing nonreciprocity [i.e., an increase of the difference between the solid red and dashed blue lines in Fig. 6(b)]. However, for lattice constants smaller than $a = 100$ μm a decrease of the band gap shift is observed although the nonreciprocity is still meaningful close to 100 μm. This is due to two effects. The first is the decrease of the nonreciprocity of the dispersion relation due to the finite conductivity and finite separation of the metal ovelayer. The second is a decrease of the group velocity of the magnonic branch that is not affected by the metal. For MCs with lattice constant smaller than $a = 73$ μm (point d in Fig. 6) the shift is decreasing rapidly, since the nonreciprocity effect disappears at large wave vectors. Thus, we can conclude that the maximal shift of the frequency band gap due to contact with the metallic film is at the value of lattice constant a for which the first Brillouin zone boundary (π/a) is close to the wave number value where in homogeneous YIG film the nonreciprocity is largest.

Finally we would like to point out four conditions required for an experimental observation of the magnonic band gaps in the metalized MCs, which can also explain the discrepancy between results presented here and in Ref. [18]. The first condition is a constant separation between the MC and the metallic screen. If the nonuniformity of the spacer thickness t throughout the structure area is significant, the band gap size might decrease or even disappear completely due to variation of the wave vector at which the Bragg resonance appears in various areas of the MC. This effect is not critical for samples presented in this paper, due to the large ratio of grooves depth to thickness, but it can cause closing of the gap for structures presented in Ref. [18]. As discussed in Ref. [18], the separation between metal and the structure might vary in the range 0–30 μm in ambient conditions. The second condition is a sufficient lateral size of the metallic screen. The wavelength (λ^+) of the incident SSW supported by a metalized surface at wave numbers close to the Bragg resonance condition is larger than in an un-metalized MC due to the pronounced shift of the edge of the magnonic band gap in the metalized structure from the border of the Brillouin zone [see Figs. 3(e) and 5(e)]. In Ref. [18] $\lambda^+ \approx 0.12$ cm is comparable with the length of the metal screen $S \approx 0.35$ cm. Thus one can expect that efficiency of the distributed Bragg mirror drops under the condition that S be of order λ. The third condition is sufficient propagation length of SSWs related to the damping and group velocity. The decrease of group velocity for large k results in the increase of propagation losses. This leads to decrease of the relative resonance of the coupling waves at the Bragg condition [35–37]. This influence is observed in Ref. [18] for samples with $t \approx 100$ μm where damping destroys transmission and the Bragg resonance. The last condition is avoiding back-voltage generation. Absence of the band gap in the metalized structures in Ref. [18] might be due to induced rf currents (directly by transducer or indirectly by SSW) in the metallic overlayer which was not grounded. A similar effect of back-voltage generation on the observation of the magnonic band gap in shorted metallic grids was already studied experimentally in Ref. [38].

In summary, we have studied transmission of the surface spin waves in one-dimensional yttrium-iron-garnet film based magnonic crystals placed near a metal screen under conditions when incident and reflected waves have nonreciprocal dispersion $f(k) \neq f(-k)$. We have proved experimentally previous theoretical findings that nonreciprocity of surface spin waves does not prevent formation of the gaps in the magnonic spectra of the metalized magnonic crystal. Due to nonreciprocity the shifts of the magnonic band gaps to higher frequency and from the border of the Brillouin zone were detected. Numerical calculations based on COMSOL software show very good agreement with experimental measurements of the magnonic band-gap shift Δf, band-gap width ΔF, and dispersion characteristics. The value of the frequency shift Δf of the magnonic gap depends on the magnonic crystal lattice constant, and on the magnetic film and dielectric spacer thicknesses. For magnonic crystals based on typical yttrium-iron-garnet films, shift of the magnonic gap can be $\Delta f > 100$ MHz and up to several times greater than the width of magnonic gap. From these last circumstances one can conclude that nonreciprocal waves are promising for manipulation of the spin wave band structure in magnonic crystals and for microwave signal processing.

We acknowledge financial assistance from the European Community, Grant No. FP7/2007-2013 under GA 247556 (People) NoWaPhen, from the National Science Centre of Poland, Project DEC-2-12/07/E/ST3/00538, from the Russian Foundation for Basic Research (13-07-00941-a, 14-07-00896-a, and 13-07-12421-ofi-m) and from the Grant of the Ministry of Education and Science of the Russian Federation (State Contract No. 11.G34.31.0030).

[1] R. W. Damon and J. R. Eshbach, J. Phys. Chem. Solids **19**, 308 (1961).
[2] M. Mruczkiewicz and M. Krawczyk, J. Appl. Phys. **115**, 113909 (2014).
[3] S. R. Seshadri, Proc. IEEE **58**, 506 (1970).
[4] R. E. De Wames and T. Wolfram, J. Appl. Phys. **41**, 5243 (1970).
[5] A. G. Veselov, S. L. Vysotskiy, G. T. Kazakov, A. G Sukharev, and Yu. A. Filimonov, J. Commun. Technol. Electron. **39**, 102 (1994).
[6] W. L. Bongianni, J. Appl. Phys. **43**, 2541 (1972).
[7] M. Uehara, K. Yashiro, and S. Ohkawa, J. Appl. Phys. **54**, 2582 (1983).
[8] O. S. Yesikov, N. A. Toloknov, and Yu. K. Fetisov, Radiotekhnika I Elektronika **25**, 1286 (1980).
[9] M. Daniel, J. Adam, and P. Emtage, Circ. Syst. Signal Process. **4**, 115 (1985).
[10] R. Marcelli, S. Nikitov, Y. A. Filimonov, A. A. Galishnikov, A. V. Kozhevnikov, and G. M. Dudko, IEEE Trans. Magn. **42**, 1785 (2006).
[11] M. Krawczyk and H. Puszkarski, Acta Phys. Pol. A **93**, 805 (1998).

[12] S. Neusser, B. Botters, and D. Grundler, Phys. Rev. B **78**, 054406 (2008).
[13] S. Tacchi, B. Botters, M. Madami, J. W. Kłos, M. L. Sokolovskyy, M. Krawczyk, G. Gubbiotti, G. Carlotti, A. O. Adeyeye, S. Neusser, and D. Grundler, Phys. Rev. B **86**, 014417 (2012).
[14] M. Krawczyk and D. Grundler, J. Phys.: Condens. Matter **26**, 123202 (2014).
[15] A. Barman and A. Haldar, in *Solid State Physics*, edited by R. Stamps and R. Camley (Elsevier, Amsterdam, 2014), Vol. 65.
[16] A. Chumak, A. Serga, S. Wolff, B. Hillebrands, and M. Kostylev, J. Appl. Phys. **105**, 083906 (2009).
[17] A. Chumak, A. Serga, S. Wolff, B. Hillebrands, and M. Kostylev, Appl. Phys. Lett. **94**, 172511 (2009).
[18] E. N. Beginin, Y. A. Filimonov, E. S. Pavlov, S. L. Vysotskii, and S. A. Nikitov, Appl. Phys. Lett. **100**, 252412 (2012).
[19] M. L. Sokolovskyy, J. W. Klos, S. Mamica, and M. Krawczyk, J. Appl. Phys. **111**, 07C515 (2012).
[20] M. Mruczkiewicz, M. Krawczyk, G. Gubbiotti, S. Tacchi, Y. A. Filimonov, D. V. Kalyabin, I. V. Lisenkov, and S. A. Nikitov, New J. Phys. **15**, 113023 (2013).
[21] M. Inoue, A. Baryshev, H. Takagi, P. B. Lim, K. Hatafuku, J. Noda, and K. Togo, Appl. Phys. Lett. **98**, 132511 (2011).
[22] V. V. Kruglyak, S. O. Demokritov, and D. Grundler, J. Phys. D: Appl. Phys. **43**, 264001 (2010).
[23] A. Khitun, M. Bao, and K. L. Wang, J. Phys. D: Appl. Phys. **43**, 264005 (2010).
[24] X. Zhang, T. Liu, M. E. Flatté, and H. X. Tang, Phys. Rev. Lett. **113**, 037202 (2014).
[25] R. Verba, V. Tiberkevich, E. Bankowski, T. Meitzler, G. Melkov, and A. Slavin, Appl. Phys. Lett. **103**, 082407 (2013).
[26] A. V. Chumak, V. S. Tiberkevich, A. D. Karenowska, A. A. Serga, J. F. Gregg, A. N. Slavin, and B. Hillebrands, Nat. Commun. **1**, 141 (2010).
[27] S. Nikitov, S. Vysotskij, A. Dzhumaliev, E. Pavlov, Y. Filimonov, and Y. Khivintsev, Russian Federation Patent No. RU2454788(C1), Byull. Izobret. **18** (2012) [in Russian].
[28] S. Vysotskii, E. Beginin, S. Nikitov, E. Pavlov, and Y. A. Filimonov, Tech. Phys. Lett. **37**, 1024 (2011).
[29] S. Vysotskii, S. Nikitov, E. Pavlov, and Y. A. Filimonov, J. Commun. Technol. Electron. **58**, 347 (2013).
[30] G. Raju, *Antennas and Wave Propagation* (Pearson Education, Boston, 2006).
[31] A. Gurevich and G. Melkov, *Magnetization Oscillations and Waves* (CRC Press, Boca Raton, 1996).
[32] M. Schäfer, *Computational Engineering – Introduction to Numerical Methods* (Springer, Berlin, 2006).
[33] F. Cardarelli, *Materials Handbook: A Concise Desktop Reference* (Springer, Berlin, 2008).
[34] Y. Filimonov and Y. Khivintsev, J. Comm. Technol. Electron. **47**, 910 (2002).
[35] Y. V. Gulyaev, S. A. Nikitov, and V. P. Plesskii, Radiotechnika I Elektronika **26**, 2282 (1981) [in Russian].
[36] S. Seshadri and M.-C. Tsai, J. Appl. Phys. **52**, 6401 (1981).
[37] S. Olivier, H. Benisty, C. Weisbuch, C. Smith, T. Krauss, and R. Houdre, Opt. Express **11**, 1490 (2003).
[38] M. Dokukin, K. Togo, and M. Inoue, J. Magn. Soc. Jpn. **32**, 103 (2008).